

Analysis of Microelectrode Arrays for Dielectrophoresis using the Finite Element Method

V. Novickij, J. Novickij, V. Stankevic, A. Grainys, S. Tolvaisiene

Vilnius Gediminas Technical University, Faculty of Electronics,

Naugarduko str., 41, LT-03227, Vilnius, Lithuania, phone: +370 5 2744762, e-mail: elektrotechnika@vgtu.lt

crossref <http://dx.doi.org/10.5755/j01.eee.118.2.1167>

Introduction

Dielectrophoresis (DEP) is a widely used separation technique for polar or polarizable particles based on the movement of the sample species which occurs when the particles are subjected to a non-uniform electric field [1]. The work presented is focused on the analysis of the DEP force distribution at nanoscale heights above the electrodes dependence on microelectrode size parameters. Results of the investigation may already find application in the fabrication of microfluidic lab on chip devices to separate or control motion of the particles in nanometer scale microfluidic channels [2]. DEP force theoretical analysis was performed using the finite element method and the dependence on microelectrode width, spacing and thickness was acquired. The electrode structure modelled was the interdigitated golden electrodes with thin Cr adhesion layer on glass substrate. Research results are applicable for any microelectrode structure that inherits rectangular structure of single microelectrode finger in its design. Using numerical calculations the influence on the gradient of electric field of each microelectrode's size parameter when the other two size parameters are altered was investigated. Taking into account resultant data, respective microelectrode structure design adjustments for future fabrication were discussed. DEP force dependence on electrode size parameters plots and research conclusions are also presented in this work.

Mathematical analysis

Dielectrophoresis (DEP) is a phenomenon that takes place when a polar or polarizable particle, e.g., a biological cell is being subjected to a non-uniform electric field which results in the motion of the particle [3,5]. This technique is widely used to characterize and separate polarizable particles. Particle range can vary from micrometer to nanometer size dimensions [6]. The DEP force affecting the specimen is produced because of the

interaction between particle dipole moment m (permanent or induced) and the non-uniform electric field [6]. The force is defined as [6]

$$F = (m\nabla)E, \quad (1)$$

where ∇ is the gradient of the electric field E .

Dipole moment m is defined as [5]

$$m = \rho v E = 4\pi \varepsilon_m F_{CM} R^3 E, \quad (2)$$

where ρ is the effective polarizability of the particle, v is the volume, ε_m is the absolute permittivity of the medium, F_{CM} is the Clausius-Mossotti factor and R is the radius of the particle [6].

From (1) and (2) DEP force is given by [6]

$$F = \rho v (E \cdot \nabla) E = 2\pi \varepsilon_m R e(F_{CM}) R^3 \nabla |E|^2. \quad (3)$$

Clausius-Mossotti factor F_{CM} is defined as [6]

$$F_{CM} = \frac{\varepsilon_p^* - \varepsilon_m^*}{\varepsilon_p^* + 2\varepsilon_m^*}, \quad (4)$$

where ε_p , ε_m are the relative permittivity of the particle and the medium, respectively. Positive F_{CM} value refers to a positive DEP when the particle is attracted to the electrodes, negative F_{CM} refers to the negative DEP and the particle is repelled from the electrodes [6]. A transition from one type of DEP to another may occur when the frequency is being altered. The frequency when the transition occurs is the crossover frequency and is defined as [6]

$$f_{x0} = \frac{1}{2\pi \varepsilon_0} \left(\sqrt{\frac{(\sigma_m - \sigma_p)(\sigma_p - 2\sigma_m)}{(\varepsilon_p - \varepsilon_m)(\varepsilon_p - 2\varepsilon_m)}} \right). \quad (5)$$

From (3) it can be seen that one of the most crucial parameters affecting the DEP force is the gradient of electric field. Therefore, the DEP force will strongly

depend on the microelectrode structure. In this work interdigitated electrode structure is analysed and the influence of the microelectrode size parameters on $\nabla|E|^2$ is investigated. The other important parameter is the Clausius-Mossotti factor F_{CM} . However, it depends only on the relative permittivities of the particle and the medium. Therefore, analysis of this parameter will not be discussed in this paper.

Numerical analysis

The electrode structure chosen for the analysis to be performed is the interdigitated electrode structure. Microelectrode width, height and thickness have been altered and respective $\nabla|E|^2$ distributions have been calculated using the finite element method [7,8]. Data analysis was performed using MATLAB software package. The interdigitated microelectrode structure that was used for numerical analysis is shown in Fig. 1.



Fig. 1. Interdigitated microelectrode structure used for numerical analysis

Microelectrode array's one connection is connected to a AC voltage source and the other to virtual earth. An electric field is formed between the electrode fingers. All theoretical simulations were performed using 3V peak-to-peak voltage. Size parameters of each electrode finger have been altered. Microelectrode finger width and spacing have been altered in the range of 5 to 20 μm . The influence of the electrode thickness on the $\nabla|E|^2$ distribution has been investigated with thickness values varying in the range of 100 to 200 nm. A 0 – 300 nm height range above the electrodes was investigated. The range of heights was selected in accordance with the widely spread optical techniques such as total internal reflectance fluorescence microscopy used for analysis of nanoscale surface events [9]. The influence of one size parameter on the gradient of electric field when the other two parameters are altered has also been investigated. Size parameter reduction steps have been chosen accordingly to include commonly used electrode model dimensions.

Simulation and modeling data that was acquired during the investigation using finite element method is applicable for all electrode types that exhibit similar edges or rectangular structure of its fingers.

The basic resultant plot of the electric field gradient distribution with applied voltage after using numerical methods is shown in Fig. 2. It can be seen that the highest gradient of the electric field is present at the tip of the electrodes. Moreover, it can also be noted from the image

that reducing the width of the electrode fingers will result in a more uniform electric field gradient throughout the whole microelectrode array designed for dielectrophoresis.

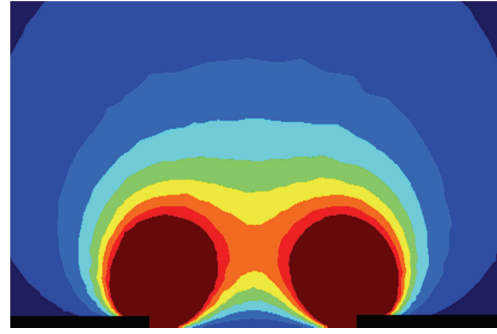


Fig. 2. Resultant plot of the electric field gradient distribution with applied voltage after using numerical methods

Different colors represent different field gradient intensity in the area near the electrodes. The gradient of electric field is higher in the area that is closer to the electrodes under investigation and colored in red, while lower gradient areas are colored in blue.

DEP force dependence on electrode width

In Fig. 3 $\nabla|E|^2$ distribution dependence on electrode width is shown. The highest gradient values were obtained using 5 and 10 μm width electrodes. The 5 μm width model showed an average 54.1 % increase of the gradient values compared to the 20 μm electrode model.

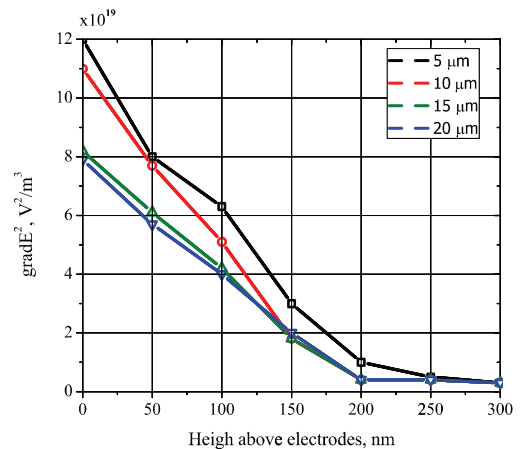


Fig. 3. $\nabla|E|^2$ distribution dependence on electrode width

It is also noticeable that there is almost no difference in the gradient values above the 200 nm heights above the microelectrodes. The 10 μm width electrodes showed a 24 % increase of the $\nabla|E|^2$ values compared to the 20 μm width model. The difference between 15 and 20 μm width microelectrodes is lower than 3 %. Therefore, the electrode width influence on the gradient of the electric field is not linear. $\nabla|E|^2$ increase rate values are taken as averages on the whole 0 – 300 nm height above the electrodes.

DEP force dependence on electrode spacing

Reduction of electrode spacing showed a similar

tendency, however, the increment rates of the gradient of electric field were a lot higher. The wider 20 and 15 μm spacing electrode arrays resulted in the lowest gradient values. The difference between these models is 58 %, which makes the reduction of the spacing between the electrodes a lot more effective than reduction of electrode width. The 10 μm width microelectrode structure showed an average increase of the gradient values by 161 % compared to the 20 μm spacing model. Same as in the width alteration analysis case, 5 μm spacing resulted in the highest gradient values. There was an average increase by 408 % of $\nabla|E|^2$ compared to the 20 μm spacing electrode version. In Fig. 4 a plot summarizing the $\nabla|E|^2$ distribution dependence on electrode spacing is shown. It is also noticeable that the influence of spacing alteration on the gradient is nonlinear.

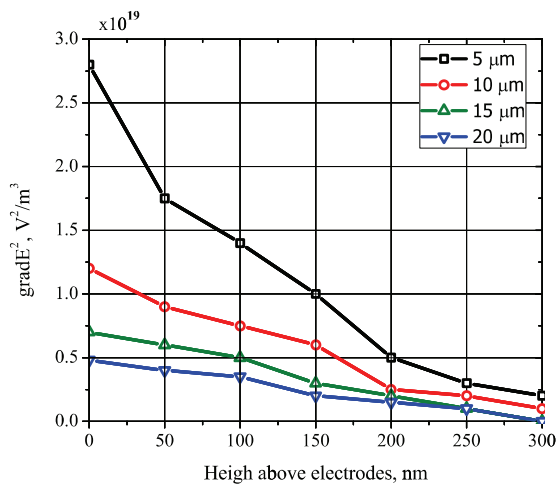


Fig. 4. $\nabla|E|^2$ distribution dependence on electrode spacing

Reduction of electrode spacing theoretically proved to be effective on the overall range of heights above electrodes that are being analyzed.

DEP force dependence on electrode thickness

$\nabla|E|^2$ distribution dependence on electrode thickness is shown in Fig. 5.

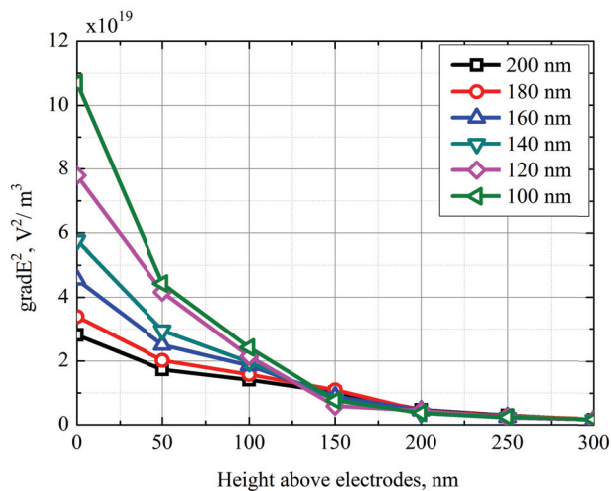


Fig. 5. $\nabla|E|^2$ distribution dependence on electrode thickness

As it is shown in Fig. 6 the highest gradient was achieved using the 100 nm thickness electrodes. However, according to numerical calculations, alteration of electrode thickness is effective only in the 0 – 100 nm range of heights. Above this height range reduction of thickness has negative or no effect on the gradient of electric field. The average increase rate of the gradient between the 100 and 200 nm thick electrode models reaches 130 %. The 180 nm thickness microelectrode structure showed an average increase of $\nabla|E|^2$ by 14 %. The difference in the gradient values between the 160 nm and 200 nm thickness models is 32 %. A tendency can be observed that with the thinner electrodes the higher gradient of electric field can be obtained in the 0 – 100 nm range of heights. The 140 nm and 120 nm electrode models resulted in the increase of $\nabla|E|^2$ by 38% and 82 %, respectively. It is noticeable that the influence of electrode thickness reduction on the gradient is nonlinear.

The plot summarizing the influence of electrode size parameters on $\nabla|E|^2$ at different height ranges is shown in Fig. 6. It can be observed that in the given range of heights the most effective way to increase the gradient of electric field and DEP force respectively is to reduce the spacing between the electrodes. Reduction of electrode thickness is effective only in the 0 – 150 nm range of heights. Moreover, in this range of heights thickness reduction is more beneficial than width alteration of the electrodes. The width reduction according to numerical calculations is effective in the 0 – 300 nm range of heights, however, the increment rates of the $\nabla|E|^2$ are low and in some cases the benefit is negligible.

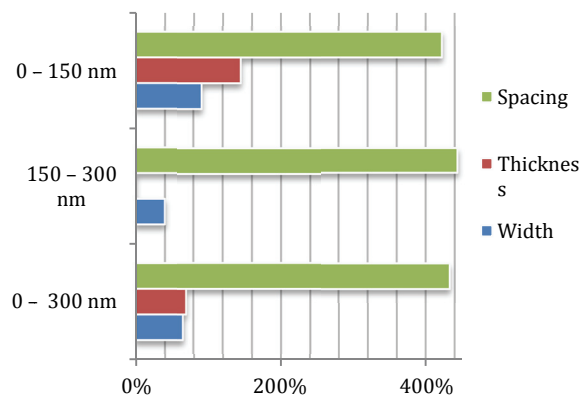


Fig. 6. Plot of the influence of electrode size parameters on $\nabla|E|^2$ at different height ranges and increase of $\nabla|E|^2$ in comparison to 20 μm width and spacing, 200 nm thickness electrodes

Using the same analysis techniques influence of one size parameter on $\nabla|E|^2$ when the other two are altered has been analyzed. It was determined that at specific heights different thickness and width combinations can result a 30 % increase of the width influence on the $\nabla|E|^2$. The alteration of the electrodes spacing had a stronger impact on the width influence on the $\nabla|E|^2$. The bigger spacing of the electrode's was selected the bigger the influence of the electrode's width was on the $\nabla|E|^2$. The use of the 5 μm

electrode's spacing resulted in the almost complete disappearance of the electrodes width influence on the $\nabla|E|^2$. The influence of electrode spacing reduction on the gradient of electric field is not strongly dependent on the other two size parameters and can be negligible. Alteration of the electrode thickness is also independent from the influence of other two size parameters. Therefore, only when electrode width is reduced other size parameters should be taken into account due to the fact they so strongly affect the effectiveness of width reduction. Moreover, as it was mentioned above reducing width of the electrode fingers results in a more uniform gradient of electric field across the whole microelectrode array.

Conclusions

DEP force theoretical analysis was performed using the finite element method and the dependence on microelectrode width, spacing and thickness was acquired. The research results are applicable for any microelectrode structure that inherits rectangular structure of single microelectrode finger in its design. It was determined that the strongest influence on the DEP force has the spacing alteration between the electrodes. The wider the spacing is, the lower DEP force will be obtained. Spacing reduction also proved to be effective on the whole range of heights that were investigated. Reduction of microelectrode structure width parameter resulted in a steady increase of the gradient of electric field. However, the increment rates are lower by a factor of 10 compared to the effectiveness of spacing reduction. Also a strong dependency of width alteration on other two parameters has been observed. Reduction of width below 10 μm when the spacing of the electrodes is less than 5 μm doesn't have any impact on the $\nabla|E|^2$. Thickness reduction proved to be effective in order to increase DEP force only in the 0 – 100 nm range of heights. However, thickness alteration effectiveness is independent from the influence of the other two parameters. Results obtained in this work may already find

application in the fabrication of microfluidic lab on chip devices to separate or control motion of the particles in nanometer scale microfluidic channels. Also the data obtained from numerical calculations can be used in order to create the most suitable electrode array design for nanoparticle separation applications where a specific DEP force value is required.

References

1. Pimbley D. W., Patel P. D., Robertson C. J. Dielectrophoresis // *Methods in Biotechnology*, 1999. – Vol. 12. – P. 35–53.
2. Giannitsis A. T., Parve T., Min M. Integration of Biosensors and Associated Electronics on Lab-on-Chip Devices // *Electronics and Electrical Engineering*. – Kaunas: Technologija, 2011 – Nr. 4(110). – P. 61 – 67.
3. Ngoc-Duy Dinh, Cheng-Hsien Liu A Lab-on-Chip for Separating and Focusing Bioparticles via Dielectrophoresis // *IFMBE Proceedings*, 2010. – P. 308–311.
4. Shafiee H., Caldwell J. L., Sano M. B., Davalos R. V. Contactless dielectrophoresis: a new technique for cell manipulation // *Biomedical Microdevices*, 2009. – P. 997–1006.
5. Nastruzzi C., et al. Applications of Dielectrophoresis-based Lab-on-a-chip Devices in Pharmaceutical Sciences and Biomedicine // *Integrated Circuits and Systems, CMOS Biotechnology, Part II*, 2007. – P. 145–178.
6. Pethig R. Cell Physiometry Tools based on Dielectrophoresis // *BioMEMS and Biomedical Nanotechnology*, 2007. – P. 103–126.
7. Novickij V. Microelectrode arrays for dielectrophoresis studies of nanoparticles, Msc. Thesis. – University of Edinburgh, Edinburgh, 2011. – P. 1–50.
8. Tarvydas P., Noreika A. Usability Evaluation of Finite Element Method Equation Solvers // *Electronics and Electrical Engineering*. – Kaunas: Technologija, 2007. – No. 2(74). – P. 13–16.
9. Giraud G., Pethig R., Schulze H., et al. Dielectrophoretic manipulation of ribosomal RNA // *Biomicrofluidics* 5, 2011. – P. 1–16.

Received 2011 10 24

Accepted after revision 2011 12 17

V. Novickij, J. Novickij, V. Stankevic, A. Grainys, S. Tolvaisiene. Analysis of Microelectrode Arrays for Dielectrophoresis using the Finite Element Method // *Electronics and Electrical Engineering*. – Kaunas: Technologija, 2012. – No. 2(118). – P. 17–20.

Dielectrophoresis (DEP) force dependence on microelectrode array size parameters is presented in this work. Using finite element method numerical calculations for golden interdigitated electrodes have been performed and DEP force at nanometer heights dependence plots were made. Using theoretical modelling microelectrode width, spacing and thickness has been altered and gradient of electric field dependence plots have been analyzed. It was showed that electrode spacing reduction is the most effective way to achieve higher DEP forces. Also the influence of one size parameter on the gradient of electric field when the other two size parameters are being altered has been studied. It was determined that reduction of width below 10 μm when the spacing of the electrodes is less than 5 μm doesn't have any impact on the gradient of electric field. Ill. 6, bibl. 9 (in English; abstracts in English and Lithuanian).

V. Novickij, J. Novickij, V. Stankevič, A. Grainys, S. Tolvaišienė. Dielektroforezės mikroeletrodų masių analizė baigtinių elementų metodu // *Elektronika ir elektrotechnika*. – Kaunas: Technologija, 2012. – Nr. 2(118). – P. 17–20.

Baigtinių elementų metodu nagrinėjama dielektroforezės jėgos priklausomybė nuo mikroeletrodų dydžio parametru. Darbe gautos dielektroforezės jėgos priklausomybės nuo mikroeletrodų pločio, tarpo ir aukščio. Sudaryti atitinkami priklausomybių grafikai ir atliktą jų analizę. Nagrinėjamos elektrodų struktūros, kurių ilgis ir tarpas tarp elektrodų keičiamas nuo 5 iki 20 mikrometru, elektrodų masyvo aukštis keičiamas nuo 100 iki 200 nanometru. Parodyta, kad mikroeletrodų tarpo keitimas yra efektyviausias būdas elektrinio lauko gradientui didinti. Taip pat išnagrinėta kiekvieno dydžio parametro įtaka dielektroforezės jėgai, kai kiti du dydžio parametrai yra keičiami. Gautas atitinkamos priklausomybės ir padarytos išvados. Parodyta, kad elektrodų aukščio ir tarpo keitimas turi įtakos pločio keitimo efektyvumui. Taikant baigtinių elementų metodą, parodyta, kad, esant mažesniai negu penkių mikrometru elektrodų tarpui, didesnis nei 10 mikrometru pločio mažinimas neturi įtakos dielektroforezės jėgai. Il. 6, bibl. 9 (anglų kalba; santraukos anglų ir lietuvių k.).